PROCEEDINGS, Thirty-Seventh Workshop on Geothermal Reservoir Engineering
Stanford University, Stanford, California, January 30 - February 1, 2012
SGP-TR-194

FULLY-IMPLICIT FLOW AND GEOMECHANICS MODEL: APPLICATION FOR ENHANCED GEOTHERMAL RESERVOIR SIMULATIONS

Perapon Fakcharoenphol, Litang Hu, and Yu-Shu Wu

Colorado School of Mines
1500 Illinois Street
Golden, CO, 80401, USA
e-mail: pfakchar@mymail.mines.edu

ABSTRACT

In recent years, enhanced geothermal system (EGS) has taken the center stage in the international community in search of future renewable energy resources. However, there is the growing public concern on EGS-induced earthquakes. Many commercial EGS fields (Basel in Switzerland, Landau in Germany, Berlin in El Salvador, etc.) have reported increasing seismic activities once the production and injection started. As a result, earthquake risk assessment is vital for EGS developments.

Fluid production and cold-water injection will alter pressure and temperature state in geothermal reservoirs. Consequently, this combined effect causes rock deformation and failure, creating underground seismic activities. Moreover, the deformation leads to the change in hydraulic properties, such as porosity and permeability, which affects fluid flow and heat transfer. To capture such physical processes, coupled effects need to be considered for the analysis of fluid flow, heat transfer, and mechanic responses.

This paper presents a numerical model of a fully coupled, fully implicit flow-geomechanics model for fluid and heat flow in porous media. The simulated stress and strain can be used to perform shear slip analysis. The developed simulator is built on TOUGH2 (Pruess et al, 1999), a well-established simulator for geo-hydrological-thermal analysis with multiphase, multi-component fluid and heat flow. We employ the staggered grid system, where the flow related primary variables (p, T, S) are located at the center of simulation grid blocks and the geomechanics related variables (ux, uy, uz) are located at the edge.

The numerical scheme is successfully verified against the analytical solution of Mandel and Cryer problem for transversely isotropic poroelastic media (Abousleiman et al., 1996) and against the published numerical results of a field-application geothermal reservoir simulation (Rutqvist et al., 2008). In addition, we present an application example for a 5-spot EGS model.

INTRODUCTION

The growing public concern on EGS-induced earthquakes causes delay of and threatens EGS development worldwide. At least one commercial EGS project (Deep heat mining Basel in Switzerland), has been abandoned because of induced felt earthquakes (Giardini, 2009). Many other commercial EGS fields (Landau in Germany, Berlin in El Salvador) and a conventional geothermal field (The Geysers) have reported increasing seismic activities once the production and injection started (Majer et al.; 2007, Giardini; 2009). As a result, site selection including earthquake risk assessment is vital for the development of geothermal fields, especially for a field that locates in suburb areas.

Production and injection activities alter pressure, temperature, and the stress state in geothermal reservoirs, which can cause rock deformation, even failure to increase seismicity or activate micro-earthquake (MEQs) events. For example, many studies have demonstrated that MEQs at The Geysers, one of the largest geothermal fields in the world, are associated with water injection and steam extraction (Oppenheimer, 1986; Stark, 2003; Smith et al., 2000; Mossop, 2001; Majer and Peterson, 2005; Majer et al., 2007). Majer et al. (2007) report the correlation between water injection rate and seismic events for the magnitude lower than 1.5, see **Fig. 1**. Rutqvist et al. (2006, 2007, and 2008) conducted a comprehensive simulation study to simulate the production and injection effects to the stress changes in The Geysers. Their results indicate that steam extraction could cause seismic activity at shallow depth above the geothermal reservoir, whereas cold water injection increase seismic activities and could

extend active slip zone several hundred meters below injection zones. These results are consistent with the observed MEQs data.

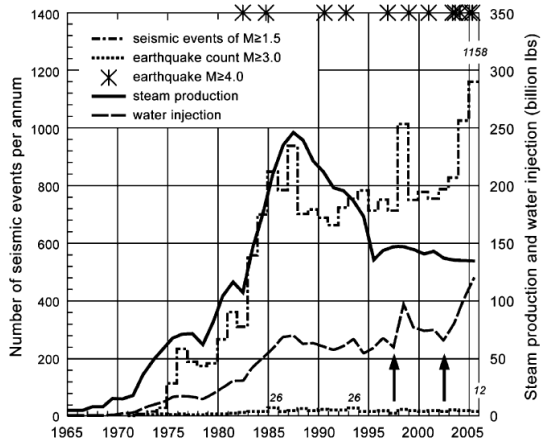

Figure 1: Historical seismicity from 1965 to 2006 at The Geysers: the two arrows indicate the increases in fluid injection in 1997 and 2002 (Majer et al., 2007)

Majer et al. (2007) point out that large earthquake risks are associated with a large fault system with significant slip. While geological information is required to evaluate the geothermal induced earthquake risks, a coupled flow-geomechanics model can be used to support the analysis on how cold water injection and steam or hot water production could affect the stress field in geothermal reservoirs in a similar manner to that of Rutqvist et al. (2006, 2007, and 2008).

Moreover, change in stress and strain induced by cold-water injection and steam extraction alter hydraulic properties, especially porosity and permeability. Many research efforts (Rutqvist et al., 2002; Davies and Davies, 1999; McKee et al., 1988; Ostensen, 1986) either experimentally or theoretically investigated the impact of rock deformation to hydraulic properties. As a result, well productivity and injectivity are changed throughout the life of wells. Thus, to evaluate production from a geothermal field, it is important to include the effect of rock deformation.

In this paper, we present a fully coupled, fully implicit flow-geomechanics model for fluid and heat flow in porous media. The simulated stress and strain can be used to perform shear slip analysis. The developed simulator is built on TOUGH2 (Pruess et al, 1999), a well-established simulator for geo-hydrological-thermal analysis with multiphase, multi-component fluid and heat flow. This simulator is not the first coupled flow-geomechanics model, but it will be among the first fully-coupled flow-geomechanics models available in public domain.

The organization of this paper is as follows. First, we briefly present the mathematical model of coupled flow-geomechanical formulation. Then, the comparison between analytical solutions and numerical results are demonstrated to show the validity of our coupling model. Furthermore, we compare our simulation results of the stress and strain analyses for production and injection induced stress changes in The Geysers to Rutqvist et al. (2006, 2007, 2008) simulation results. Finally, an application example for 5-spot EGS model is presented.

MATHEMATICAL MODEL

We develop a fully-coupled geomechanics and flow model, which is based on Charoenwongsa et al. (2010) and Shu (2003) works. We assume that boundaries of each simulation grid can move only perpendicular to its interface as an elastic material and obeys the generalized Hooke law. Three additional primary variables, namely displacement in x, y, and z direction (u_x, u_y, u_z), for each grid are introduced. Although, this numerical scheme is only applicable for Cartesian grid, it is sufficient to simulate flow and geomechanics behavior in geothermal reservoirs where the geological information as well as actual subsurface information from drilled wells is rather sparse and less dense than that of oil and gas reservoirs.

Reservoir rock is assumed under force equilibrium at all time, and the effect of acceleration of rock frame is ignored. The force equilibrium equations under Newton law can be expressed:

$$\nabla \bullet (\Delta\sigma) + \Delta\rho\vec{g} = 0 \tag{1}$$

where, $\Delta\sigma$ is tensor of total stress change from the previous equilibrium condition; here compression is positive and tension is negative, $\Delta\rho$ is average bulk density change from the previous equilibrium condition, typically this value is very small and is dominated by the change of fluid density inside pore space, $\vec{g}$ is gravity vector.

In Cartesian coordinate, Eq. (1) can be written as:

$$\begin{bmatrix} \nabla \bullet (\Delta\vec{\sigma}_x) \\ \nabla \bullet (\Delta\vec{\sigma}_y) \\ \nabla \bullet (\Delta\vec{\sigma}_z) + \Delta\rho\vec{g} \end{bmatrix} = \begin{bmatrix} 0 \\ 0 \\ 0 \end{bmatrix} \tag{2}$$

where $\vec{\sigma}_x$ is stress components vector acting in x-direction and composes of normal stress in x-plane (σ_{xx}), shear stress in y-plane (σ_{yx}), and shear stress in z-plane (σ_{zx}), $\vec{\sigma}_y$ is stress components vector acting in y-direction, and $\vec{\sigma}_z$ is stress components vector acting in z-direction.

Following the numerical framework used in TOUGH2, we can discretize Eq. (2) as follows:

$$\int_{\Gamma_n} \mathbf{F}_j \bullet \mathbf{n} d\Gamma_n + q_j = 0 \tag{3}$$

where, $\mathbf{F}_j = \left[\Delta\sigma_{xj} \quad \Delta\sigma_{yj} \quad \Delta\sigma_{zj} + \delta_{zj}\Delta\rho g\right]^T$, $j \in \{x, y, z\}$, and q_j is external force adding to the system.

Stress-Strain Relation

Using above formulation, we can include different stress-strain relationship. Here, we assume rock behaves as a linear poro-thermo-elastic medium with orthotropic material. The stress-strain relationship is given:

$$\begin{bmatrix} \Delta\sigma_{xx} - \alpha_x\Delta p \\ \Delta\sigma_{yy} - \alpha_y\Delta p \\ \Delta\sigma_{zz} - \alpha_z\Delta p \\ \Delta\sigma_{xy} \\ \Delta\sigma_{yz} \\ \Delta\sigma_{zx} \end{bmatrix} = \begin{bmatrix} \frac{1}{E_x} & -\frac{\nu_{yx}}{E_y} & -\frac{\nu_{zx}}{E_z} & 0 & 0 & 0 \\ -\frac{\nu_{xy}}{E_x} & \frac{1}{E_y} & -\frac{\nu_{zy}}{E_z} & 0 & 0 & 0 \\ -\frac{\nu_{xz}}{E_x} & -\frac{\nu_{yz}}{E_y} & \frac{1}{E_z} & 0 & 0 & 0 \\ 0 & 0 & 0 & 1/G_{xy} & 0 & 0 \\ 0 & 0 & 0 & 0 & 1/G_{yz} & 0 \\ 0 & 0 & 0 & 0 & 0 & 1/G_{zx} \end{bmatrix}^{-1} \begin{bmatrix} \varepsilon_{xx} + \beta_x\Delta T \\ \varepsilon_{yy} + \beta_y\Delta T \\ \varepsilon_{zz} + \beta_z\Delta T \\ 2\varepsilon_{xy} \\ 2\varepsilon_{yz} \\ 2\varepsilon_{zx} \end{bmatrix} \tag{4}$$

where, ε_{ij} is normal strain if $i=j$ and shear strain if $i \neq j$, $i, j \in \{x,y,z\}$, E is elastic modulus, ν is passion ratio, G is shear modulus, β is linear thermal expansion, α is Biot coefficient, ΔT is temperature change, and Δp is pressure change.

Also, we assume that small strain assumption is adequately capture strain in our system. Strain can be calculated from:

$$\varepsilon_{ij} = \frac{1}{2}\left(\frac{\partial u_i}{\partial x_j} + \frac{\partial u_j}{\partial x_i}\right) \qquad i, j \in \{i, j, k\} \tag{5}$$

where, u_x, u_y, and u_z are displacement of rock frame in x, y, and z-direction, ε_{ij} is strain component.

Boundary Treatment

Three types of boundary conditions are discussed here. First, a rigid boundary describes stationary rock frame at the reference point. Second, a sliding boundary describes that the movement of a boundary face only occurs in parallel to the face of simulation grid, no movement in the perpendicular direction to the face is allowed. This type of boundary is commonly used for the outer model boundaries. The last boundary type is a specific stress boundary where a boundary is subject to a constant stress condition including normal and shear stresses. Typically, ground surface is modeled by constant zero-stress boundary. All three boundaries types can be mathematically expressed as follows:

Rigid Boundary:

$$u_x = 0, \quad u_y = 0, \quad u_z = 0 \tag{6}$$

Sliding Boundary:

$$u_i = 0, \quad \sigma_{ij} = 0 \quad i, j \in \{x, y, z\} \text{ and } i \neq j \tag{7}$$

Specific Stress Boundary:

$$q_j = \int_s C_{ij} \bullet \vec{n} ds \qquad i, j \in \{x, y, z\} \tag{8}$$

where, C_{ij} is stress component at boundary

Effect of Geomechanics on Mass and Energy Balance Equations

Rock deformation affects fluid flow in many aspects; the following section explains how we mathematically incorporate the effects.

Permeability and Porosity:

These two quantities are among the most important properties for fluid flow and can be greatly affected by rock deformation. Many research efforts (Rutqvist et al., 2002; Davies and Davies, 1999; McKee et al., 1988; Ostensen, 1986) either experimentally or theoretically investigated the impact of rock deformation to hydraulic properties. Summary of the permeability and porosity as functions of stress can be found in Wu et al. (2011). The general mathematical form can be expressed as:

$$k = k(\sigma', \varepsilon) \tag{9}$$

$$\phi = \phi(\sigma', \varepsilon) \tag{10}$$

where k is absolute permeability, ϕ is porosity, σ' is effective stress, and ε is strain.

Mass Accumulation:

The total mass within a unit volume of rock may be changed due to rock deformation. We account for the mass calculation as:

$$M^{\kappa} = \sum_{\varphi} (1-\varepsilon_v)\phi S_{\varphi}\rho_{\varphi}X_{\varphi}^{\kappa} \quad (11)$$

where, M^{κ} is mass accumulation per unit volume of component κ, ε_v is volume metric strain, ϕ is porosity, ρ_{φ} is density of phase φ, S_{φ} is saturation of phase φ and X_{φ}^{κ} is the mass fraction of component κ in phase φ.

Capillary Pressure:

Due to the change in permeability and porosity, Rutqvist et al. (2002) use J-function to correct capillary pressure change.

$$p_c = p_{c,0}\sqrt{\frac{k_0\phi}{k\phi_0}} \quad (12)$$

where, $p_{c,0}$ is non-deformed capillary pressure, k_0, k are initial permeability and deformed permeability, respectively, and ϕ_0, ϕ are initial porosity and deformed porosity, respectively,

Fluid Mass Flow Rate:

Not only intrinsic rock properties are altered, but also surface area of grid blocks is changed due to deformation. Here we include the effect.

$$q_{\varphi,i} = -F_v\frac{kk_{r\varphi}}{\mu_{\varphi}}\nabla\Phi A_0 \quad (13)$$

where F_v is deformation correction defined as $F_{v,i} = \frac{(1-\varepsilon_{jj})(1-\varepsilon_{kk})}{1-\varepsilon_{ii}}$ and $i,j,k \in \{x,y,z\}$ and $i \neq j \neq k$, A_0 is initial surface area, k is absolute permeability, $k_{r\varphi}$ is relative permeability of phase φ, and μ is viscosity of phase φ.

MODEL VERIFICATION

Mandel-Cryer Problem for Transversely Isotropic Porous Media

Classical Mandel-Cryer problem involves an infinitely long rectangular specimen, sandwiched at the top and the bottom by two rigid frictionless plates, see **Fig. 2**. The lateral sides are free from normal and shear stresses, and pore pressure. At t=0, a stress of σ is applied to the top of the rigid plates. As a result, pore pressure is uniformly increased by the Skempton effect. The pore pressure then dissipates from the side edges.

Abousleiman et al. (1996) extend the classical problem to account for transversely isotropic material. Fig. 2 shows Mandel-Cryer problem for a transverse isotropic material where a) case#1: the axis of material rotational symmetry coincides with z-axis and b) case#2: the specimen is rotated by 90˚ in y-direction.

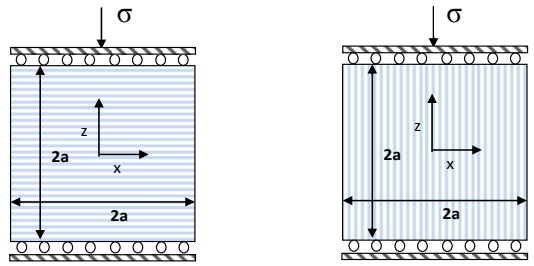

Figure 2: Problem description (a) Case#1: the axis of material rotational symmetry coincide with z-axis and (b) Case#2: the specimen is rotated by 90˚ from case#1

Table 1: Input parameters for Case#1: Mandel-Cryer problem

Parameters	Value	Unit
Young modulus in x and z directions	20.6, 17.3	GPa
Poisson ratio in xy and xz directions	0.189, 0.246	-
Biot coefficient in x and z directions	0.733, 0.749	-
Permeability x and z directions	1.0×10^{-19}, 2.0×10^{-20}	m^2
Porosity	0.1	-
Fluid viscosity	0.001	Pa.s
Pore compressibility	2.0×10^{-10}	1/Pa
Fluid compressibility	4.4×10^{-10}	1/Pa
Applied stress	10	MPa

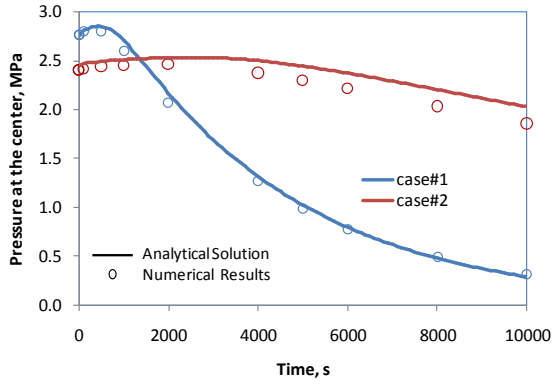

Figure 3: Comparison of pressure solutions between numerical simulation and analytical solution for (1) case#1: material properties according to Table1 and (2) Case#2: the specimen is rotated 90 from Case#1.

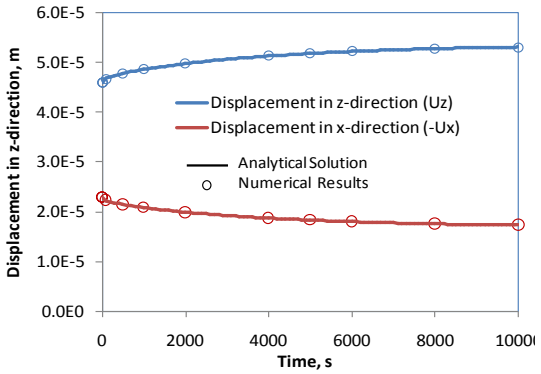

Figure 4: Comparison of displacement in x-direction at the right edge and z-direction at the top of the specimen, between numerical simulation and analytical solution for case#1.

The simulation results and analytical solution are compared in **Fig. 3** and **Fig. 4**. The figures show good agreement between the two methods; thus, it lends credibility to our numerical simulation model.

Published Simulation Results: The Geysers Geothermal-Induced Micro-Earthquake Study

In this section, we compare our simulation results (here we named our simulator 'TOUGH2-EGS') to the published simulation results of The Geysers geothermal-induced Micro-Earthquake (MEQs) Study. The study was conducted by Rutqvist et al. (2006, 2007, and 2008), to investigate effect of steam extraction and water injection in The Geysers.

The Geysers is one of the largest geothermal reservoirs in the world and located in one of the most seismically active regions, the northern California. It is a vapor-dominated geothermal reservoir system, hydraulically confined by low-permeability rock units. Many studies have demonstrated that MEQs at The Geysers associate with water injection and steam extraction (Oppenheimer, 1986; Stark, 2003; Smith et al., 2000; Mossop (2001); Majer and Peterson, 2005; Majer et al., 2007).

Rutqvist et al. (2006, 2007, and 2008) conducted a simplified two-dimensional model simulation representing one-half of a NE-SW cross-section of the NW-SE trending of The Geysers geothermal field, **Fig. 5**. The initial (pre-production) conditions were established through a steady state multi-phase flow simulation. Published data were used to constrain a conceptual Geysers model; detail model setup can be found in their papers. One producer and two injectors are located at the model center, **Fig. 6**. The steam production and water injection rates throughout 44 years history were scaled to represent the ratio of withdrawal and injection volume to the cross-section model.

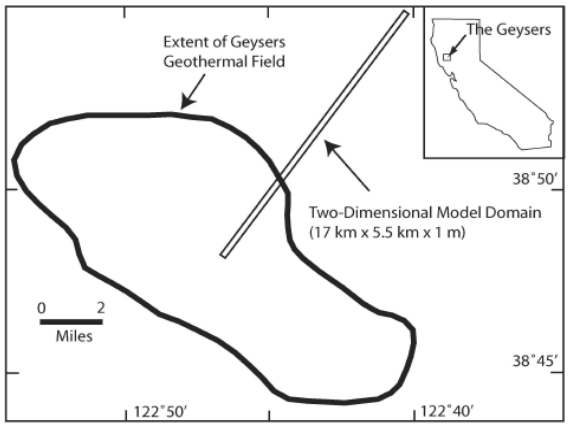

Figure 5: Schematic maps of the study area (Rutqvist and Odenburg, 2008)

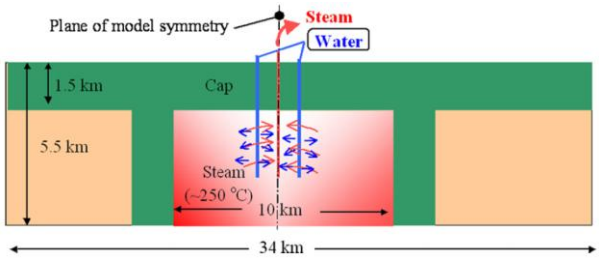

Figure 6: Model schematic: one producer and two injectors (Rutqvist et al. 2008)

The authors employed a coupled flow-geomechanics model using two separated simulators, TOUGH2 (a fluid and heat flow simulator) and FLAC (a commercial geomechanics simulator). TOUGH2 provided pressure and temperature changes to FLAC to calculate stresses changes. No stress information from FLAC was return to TOUGH2. This coupling technique is known as one-way coupling, where pressure and temperature changes influence stresses changes, but stresses changes do not affect hydraulic properties of current time steps and thus mass and energy balance calculations.

The production and injection rate history of The Geysers was scaled and used to control production and injection rate of the model. This case was setup to investigate both steam extraction and water injection effects. Detail model setup can be found in Rutqvist et al. (2006, 2007, and 2008).

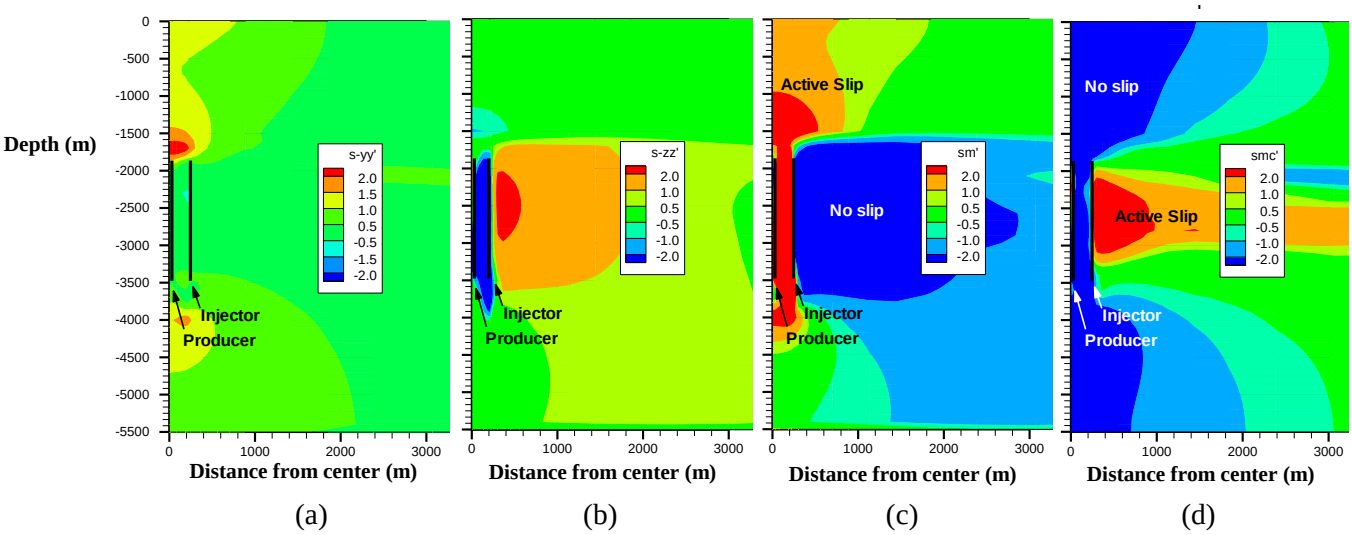

Figure 7: Simulation results using TOUGH2-EGS: (a) change in effective horizontal stress, (b) change in effective vertical stress, (c) $\Delta\sigma'_1$-$\Delta\sigma'_{1c}$ for compressional stress regime ($\sigma'_1 = \sigma'_h$) , where positive value indicates the stress change exceed the critical stress change and can activate MEQs, and (d) $\Delta\sigma'_1$-$\Delta\sigma'_{1c}$ for extensional stress regime ($\sigma'_1 = \sigma'_v$).

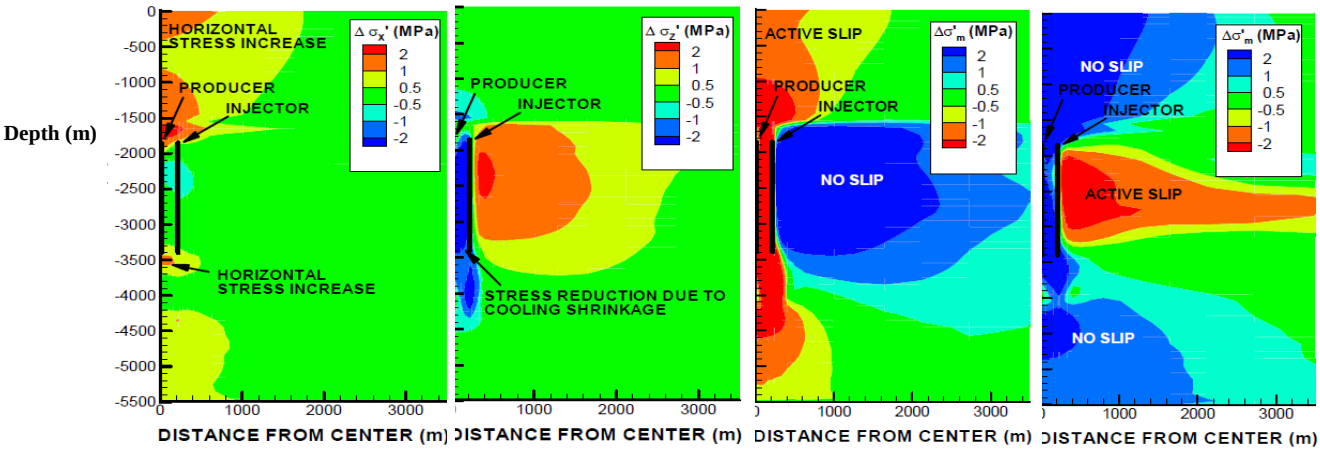

Figure 8: Rutqvist et al. (2007) simulation results: (a) change in effective horizontal stress, (b) change in effective vertical stress, (c) $\Delta\sigma'_1$-$\Delta\sigma'_{1c}$ for compressional stress regime ($\sigma'_1 = \sigma'_h$) , where positive value indicates the stress change exceed the critical stress change and can activate MEQs, and (d) $\Delta\sigma'_1$-$\Delta\sigma'_{1c}$ for extensional stress regime ($\sigma'_1 = \sigma'_v$).

Fig. 7 shows simulation results from TOUGH2-EGS. Fig. 7(a) and Fig. 7(b) depict vertical and horizontal stress changes at the center of the field, respectively. Based on Mohr-Coulomb failure criterion, the critical stress change in the maximum principal stress ($\Delta\sigma_{1c}$) is calculated as three times the change in minimum principal stress ($\Delta\sigma_3$) (Rutqvist et al., 2006). Fig. 7(c) and Fig. 7(d) show the indication of active slip or rock failure potential, where positive value indicates failure zone and negative indicates stable zone in compressional stress regime ($\sigma'_1=\sigma'_h$) and extensional stress regime ($\sigma'_1=\sigma'_v$), respectively. The simulation results indicate that steam extraction yields active slip regime in shallow depth at the reservoir cap rock for compressional stress regime, while no slip is expected in extensional stress regime. These results are consistent with that of published simulation results showed in **Fig. 8** (Rutqvist et al., 2006).

APPLICATION EXAMPLE

In geothermal reservoir development, production and injection wells are often drilled in regular geometric patterns. The present problem considers a large well field with wells arranged in a "5-spot" pattern. Because of symmetry, only a quarter of the basic pattern needs to be modeled. **Fig. 9** shows simulation grid where the grids are refined in the vicinity of injection and production wells and coarse grids are used elsewhere. The system is initialized as a normal pressure regime where subsurface pressure follows hydrostatic pressure of water head, and temperature gradient is set at 4˚C/km. The reservoir is fully saturated with water. Reservoir rock properties are corresponding to conditions that may typically be encountered in deeper zones of hot and fairly tight geothermal reservoirs.

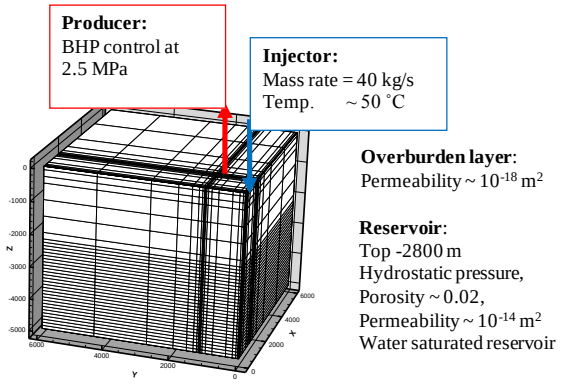

Figure 9: A quarter model for 5-spot pattern

Continuum Slip Analysis

We employed continuum shear-slip analysis to investigate the extension of potential slip zones, as discussed by Rutqvist et al. (2006). Cold-water injection and steam extraction cause pressure and temperature changes as well as alter stress field in reservoirs. To evaluate potential slip zone, the effective stress can be compared to Mohr-Coulomb failure criterion. In this case, fracture orientations must be known. However, the orientation data may not available. As precaution, we assume that preexisting fractures could rotate in any direction. Mohr-Coulomb failure criterion is given as (Jaeger et al., 2007):

$$\tau_m = S_0 \cos\theta + \sigma_m \sin\theta \qquad (14)$$

where τ_m and σ_m are the two-dimensional maximum shear stress and mean stress in the principal stress plane (σ'_1, σ'_3), defined as:

$$\sigma_m = \frac{1}{2}(\sigma'_1+\sigma'_3), \quad \tau_m = \frac{1}{2}(\sigma'_1-\sigma'_3) \qquad (15)$$

where S_0 and θ are the coefficient of internal cohesion and angle of internal friction of the fractures, respectively.

In this example the potential for shear slip is estimated using zero cohesion ($S_0 = 0$) and a friction angle of 30°, leading to the following criterion for shear slip:

$$\sigma'_1 = 3\sigma'_3 \qquad (16)$$

Thus, shear slip would be induced whenever the maximum principal effective stress exceeds three times the minimum compressive effective stress.

Simulation Results

Fig. 10 and **Fig. 11** show simulation results after 6 months of production at vicinity of the injector and producers, respectively. Around the injector, the temperature is reduced, caused by cooling effect, and causes stress reduction, as can be seen that the horizontal stress change follows the temperature change pattern, see Fig. 10(a) and (b). As a result, permeability is enhanced around the injector, Fig. 11(c). Fig. 11(d) demonstrates active slips zone for extensional regime (the maximum stress is in the vertical direction). Here, positive value indicates failure zone. It is clearly seen that failure zone evolve around the injector in both cases.

The pressure reduction caused by steam extraction dominates the stress changes around the producer, as the horizontal and vertical stress changes follow the pressure change pattern, Fig. 11 (a) and (b). Consequently, the permeability around the producer declines. Unlike, around the injector, Fig. 10 (d) indicate no active slip zone develops around the producer. As pressure reduction raise the effective normal stress around the producer, the fracture slip potential is reduced. We can see that the active slip zone is only developed around the cold-water injector. Thus, we can study the detailed evolution of the active slip zone around the injector.

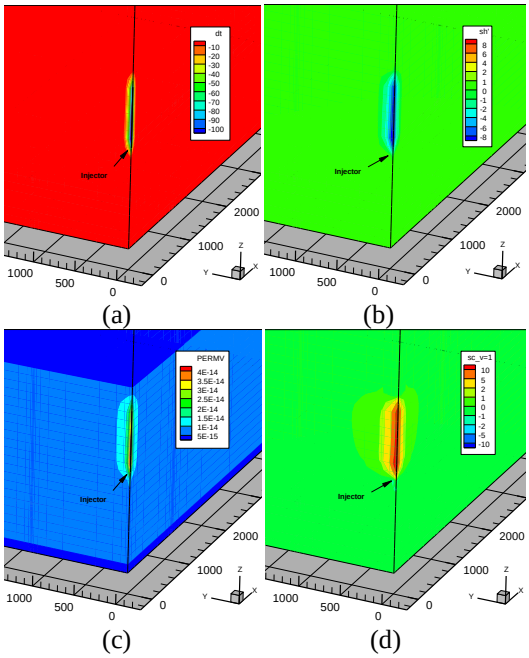

Figure 10: Simulation results at the injector after 6 months: (a) temperature change (b) horizontal stress change, (c) permeability evolution, and, (d) $\Delta\sigma'_v$-$\Delta\sigma_c$ plot for extensional stress regime where positive indicates slip zone.

Fig. 12 demonstrates active slip zone evolution around the water injector in both extensional and compressional stress regimes. Under extensional stress regime, active slip zone can extend several hundred meters above the injection point during the early production period, Fig. 12 (a). Later, the active slip zone only extends horizontally away from the injector. After five years of production, this zone could extend beyond 500 m. away from the injector, Fig 12 (c). This is because during the early production, pressure drop in the reservoir is insignificant, thus only temperature drop, causing stress reduction and dominating the stress field. As temperature change occurs locally, it creates tension zone in the vertical direction, thus extending failure zone vertically. However, after reservoir pressure drop is significant, it raises the effective stress and counteracts temperature effect. As a result, it diminishes vertical tension zone and the active slip zone only extends horizontally.

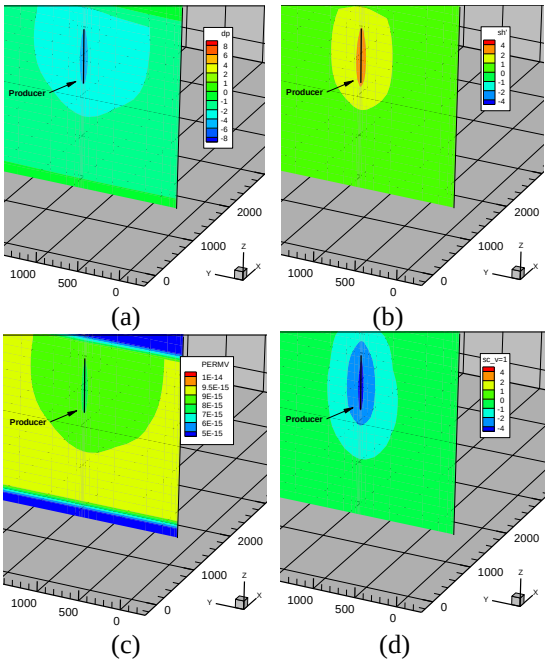

Figure 11: Simulation results at the producer after 6 months: (a) pressure change, (b) vertical stress change, (c) permeability evolution , (d) $\Delta\sigma'_v$-$\Delta\sigma'_c$ plot for extensional stress regime where positive indicates slip zone.

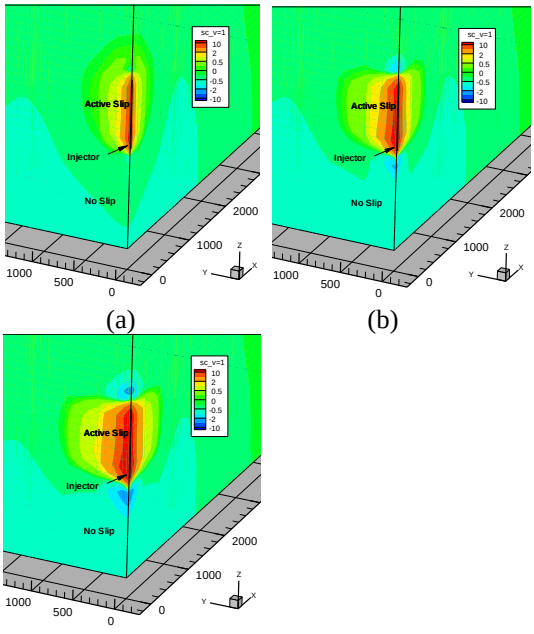

Figure 12: Slip potential plot ($\Delta\sigma'_1$-$\Delta\sigma'_{1c}$) where positive indicates active slip and negative indicates no slip zones for: extensional stress regime (maximum stress is the vertical stress) at (a) 0.5 year, (b) 1.5 year, (c) 5 years.

CONCLUSIONS

In this paper, we describe a fully coupled, fully implicit flow-geomechanics model for fluid and heat flow in porous media. The simulated stress and strain can be used to perform shear slip analysis as well as to analyze the effect of rock deformation on fluid and heat flow in geothermal reservoirs. The developed simulator is built on TOUGH2 (Pruess et al, 1999), a well-established simulator for geo-hydrological-thermal analysis with multiphase, multi-component fluid and heat flow. The developed simulator is not the first coupled flow-geomechanics simulator, however will be one of the first fully-coupled flow-geomechanics simulators available in public domain.

We successfully validated our simulator against the analytical solution of Mandel and Cryer problem for transversely isotropic poroelastic media (Abousleiman et al., 1996) and against the published numerical results of a field-application of geothermal reservoir simulation (Rutqvist et al., 2008). In addition, we present an application example for a 5-spot EGS model.

As the growing public concerns on EGS-induced earthquakes, site selection and earthquake risk assessment is vital for EGS development. Our simulator can be used to support the assessment on how cold water injection and steam or hot water production could affect the stress field and productivity in geothermal reservoirs as well as induced seismicity.

ACKOWLEDGMENTS

This work is supported by the U.S. Department of Energy under contract No. DE-EE0002762. Special thanks are due to Energy Modeling Group (EMG) and Marathon Center of Excellence for Reservoir Studies (MCERS) at Colorado School of Mines. The authors are also grateful to Jonny Rutqvist at Lawrence Berkeley National Laboratory (LBNL) for his help provided to the study.

REFERENCES

Aoki, T., Tan, C.P., and Bamford, W.E. (1993), "Effects of elastic and strength anisotropic on borehole failures in saturated rocks," *Int. J. Rock Mech. Min. Sci.*, **10**, 1031-1034.

Abousleiman, Y., Cheng, A. H.-D., Detournay, E., Cui, L., and Roegiers, J.-C. (1996), "Mandel's problem revisited," *Géotechnique*, **46**(2), 187-195.

Carslaw, H. S., Jaeger, J. C., (1986), "Conduction of heat in solids," second ed. Oxford University Press, USA.

Charoenwongsa, S., Kazemi, H., Miskimins, J. L., and Fakcharoenphol, P., (2010), "A fully-coupled geomechanics and flow model for hydraulic fracturing and reservoir engineering applications," *in proceeding of Canadian Unconventional Resources & International Petroleum Conference*, Calgary, Alberta, Canada.

Davies, J.P., Davies, D.K., (1999), "Stress-dependent permeability: characterization and modeling," *in proceeding of SPE Annual Technical Conference and Exhibition*, SPE 56813, Houston, Texas.

Giardini, D, (2009), "Geothermal Quake Risks Must be Faced," *Nature*, **462**(7275), 848-849.

Jaeger, J., Cook, N. G., and Zimmerman R., (2007), "Fundamentals of rock mechanics", forth ed. Wiley-Blackwell.

Majer, E. L., Baria, R., Stark, M., Oates, S., Bommer, J., Smith, B., and Asanuma, H., (2007), "Induced Seismicity Associated with Enhanced Geothermal Systems," *Geothermics*, **36**(3), 185-222.

Majer, E.L., and Peterson, J.E., (2005), "Application of microearthquake monitoring for evaluating and managing the effects of fluid injection at naturally fractured EGS sites," *Geotherm. Resour. Counc. Trans*, **29**, 103–107.

McKee, C.R., Bumb, A.C., and Koenig, R.A., (1988), "Stress-dependent permeability and porosity of coal and other geologic formations," *SPE Formation Evaluation*, **3**(1), 81–91.

Massachusetts Institute of Technology (MIT), (2006), "The future of geothermal energy impact of enhanced geothermal systems (EGS) on the United States in the 21st Century", *A report for the U.S. Department of Energy*.

Mossop, A.P., (2001), "Seismicity, subsidence and strain at The Geysers geothermal field", *Ph.D. dissertation*, Stanford University, Stanford, CA.

Ostensen, R.W., (1986), "The effect of stress-dependent permeability on gas production and well testing," *SPE Formation Evaluation*, **1**(3), pp. 227–235.

Oppenheimer, D.C., (1986), “Extensional tectonics at the Geysers geothermal area, California,” *J. Geophys. Res.*, **91**, 11463–11476.

Pruess, K., Oldenburg, C., and Moridis, G., (1999) “TOUGH2 user's guide, Version 2.0,” *Lawrence Berkeley Laboratory Report LBL-43134*, Berkeley, CA.

Rutqvist J., Birkholzer, J., Cappa, F., Odenburg, C.M., and Tsang, C.F., (2006), “Shear-slip analysis in multiphase fluid flow reservoir engineering applications using TOUGH-FLAC,” *in proceeding of TOUGH Symposium*, LBNL, Berkeley, California.

Rutqvist J., and Odenburg, C.M., (2007), “Technical Report#1: Development of fluid injection strategies for optimizing steam production at The Geysers geothermal field, California,” LBNL, Berkeley, California, LBNL-62577.

Rutqvist, J., and Odenburg, C.M., (2008), “Analysis of injection-induced micro-earthquakes in a geothermal steam reservoir, The Geysers geothermal field, California,” *in proceeding of The 42nd U.S. Rock Mechanics Symposium (USRMS)*, San Francisco, California.

Rutqvist, J., Wu, Y.S., Tsang, C.F., and Bodvarsson, G., (2002), “A modeling approach for analysis of coupled multiphase fluid flow, heat transfer, and deformation in fractured porous rock,” *Int. J. Rock Mech. Min. Sci.*, **39**, 429–42.

Smith, J.L.B., Beall, J.J., and Stark, M.A., (2000), “Induced seismicity in the SE Geysers field”. *Geotherm. Resour. Counc. Trans*, **24**, 24–27.

Stark, M.A, (2003), “Seismic evidence for a long-lived enhanced geothermal system (EGS) in the Northern Geysers Reservoir,” *Geotherm. Resour. Counc. Trans*, **27**, 727-731.

Shu, T., (2003), “Development of Efficient Fully Coupled Geomechanics and Fluid Flow Simulator,” *Master Thesis*, Stanford University, Stanford, CA.

Terzaghi, K., (1943), “Theoretical Soil Mechanics,” John Wiley and Sons, New York.

Wu, Y.S., Kazemi, H., Xu, T., Zhang, K., Hu, L., Zhao, X., and Fakcharoenphol, P., (2011), “Quarterly Report 2 of Year 2: Development of Advanced Thermal-Hydrological-Mechanical-Chemical (THMC) Modeling Capabilities for Enhanced Geothermal Systems,” *A report for the U.S. Department of Energy*.